First Break September '03 06-08-2003 12:19 Pagina 11

History matching using both production and 4D-4C seismic

Ali Al-Naamani and Colin MacBeth, Heriot-Watt University, Edinburgh, UK discuss some refinements to history matching in 4D seismic analysis using PS time-lapse data.

The purpose of time-lapse seismic measurement is to be able to monitor the reservoir during production or improved oil recovery by detecting induced changes in the seismic attributes. Within reservoir simulation, the aim is to develop a realistic reservoir model, which agrees with all available static and dynamic information from which we can make accurate future predictions about reservoir performance and plan further developments. Reservoir model history-matches are non-unique, more than one combination of reservoir model input parameters will match observed production. In most cases, we have an incomplete understanding of our reservoirs and how they will behave during production. However, issues such as connectivity, permeability pathways, and water encroachment will lead to large uncertainties.

We often do not know how our reservoirs will behave until we flow them. This is why time-lapse seismic should be an integral part of any field development plans. Time-lapse seismic monitoring is a valuable asset to reservoir engineering, because it provides 3D dynamic data rather than the spatially limited well test and production data. Most seismic history matching studies are achieved by constraining the reservoir model with PP time-lapse data. The aim of this work is to judge the value of incorporating PS time-lapse data as an additional constraint in the process of performing a qualitative seismic history matching.

Seismic data

The focus of this analysis is the Teal South field which is located approximately 178 miles SW of New Orleans in Eugene Island Block 354 in the Gulf of Mexico. The water bottom consists of soft unconsolidated mud at a depth of approximately 90 m. Seismic data sets covering three different times are available: one time prior to production (legacy towed streamer data acquired in 1995), and at two times during production (OBC phase I and II). Phase I was shot in July 1997 with a 25 m x 25 m shot grid over 9 km^2 using four East-West lines of six receivers at a line interval of 400 m and a receiver interval of 200 m. Phase II was acquired in April 1999 with the same acquisition extended with a shot grid area of 12 km^2 and three additional N-S lines of four receivers to the east of the original lines. The post-stack/migrated PP data for the legacy towed streamer, P-Z summed and PS data for OBC I and II were available for this study. The legacy data was processed using conventional processing flows. For the OBC, some time processing steps specific to this acquisition were undertaken – for the PP waves surface consistent compensation of coupling between receivers and the sea bottom, and P-Z summation. For PS waves surface consistent receiver statics, reorientation of the horizontal components and then asymptotic binning (Haggard, ERCH consortium meeting 2000). After processing, the target was identified on the PS data using the target-oriented correlation analysis. Although the PS sections should be differentially compressed using a range of V_p/V_s to fit all events, in our case the target event on both PP and PS could be aligned using an average V_p/V_s of 3.2.

The target is a turbidite sand at 4500 ft depth, which has also been the focus of previous work (e.g. Al-Naamani and MacBeth, 2002). The reservoir interval is made up of turbidite sheet sands bounded by faults and a dip closure to the north and has been interpreted by Alexander and Flemings (1995) as incised-valley fill deposition. Reservoir details are given in Table 1. Initial production began in November 1996, with the reservoir being initially over-pressured and close to bubble point but no pre-existing gas caps. Pressure drop due to production quickly generated a small gas cap and zone of water encroachment. From Figure 1, three time-lapse anomalies, A, B and C, can be identified on OBC P-Z summed RMS amplitude maps and the anomaly C which

Turbidite sands	Fluids
28% average porosity S_w=0.75, S_g=0.65 P_c=1414psi, P_p=799psi λhigh=6.70GPa μhigh=1.86Gpa	28° API Initial GOR 800 scf/stb Pressure phase I 2820 psi (19.2 MPa) Pressure phase II 2190 psi (14.8 MPa) Temperature 59°C
Reservoir	**Seismic**
Top reservoir: 4500 ft TVDSS	P-P: 30Hz; P-S 25Hz peak frequency Surveys: legacy 1995, OBC 1997, OBC 1999 Offset range 0-9000'

Table 1 *Rock and fluid properties for the reservoir formed by the 4500 ft sand at the Teal South field. The dry rock parameters are chosen from the database of MacBeth (2003).*

© 2003 EAGE

First Break September '03 06-08-2003 12:19 Pagina 12

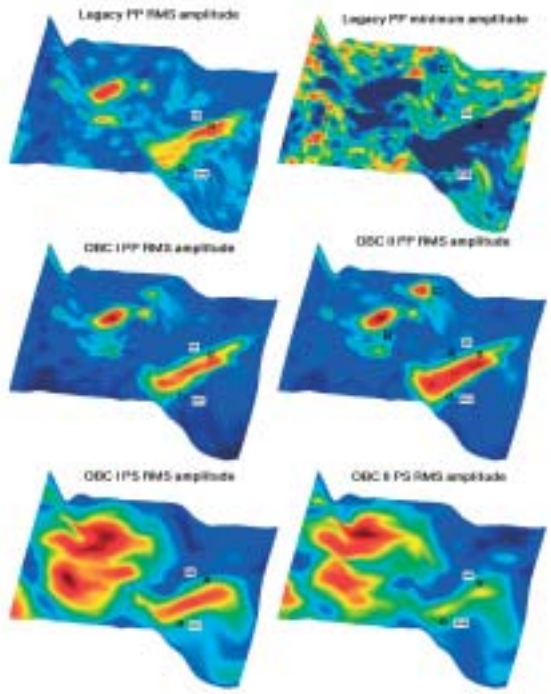

Figure 1 *PP amplitude maps for towed-streamer and PP and PS maps for OBC surveys. Time-lapse anomalies A, B and C are identified on OBC I and II. Anomaly C that cannot be seen on RMS amplitude map can now be seen on minimum amplitude map of the towed-streamer legacy data.*

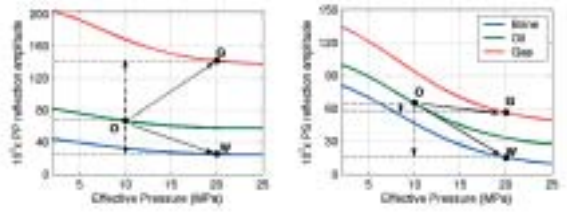

Figure 2 *Modelled PP and PS reflection amplitude for a variety of end-member reservoir changes in a 50 ft oil sand undergoing production. The saturations for gas replacing oil, oil saturated and water from aquifer replacing produced oil cases are considered (S_g=0.75, S_{org}=0.10, S_{wc}=0.15), (S_o=0.85, S_{wc}=0.15) and (S_{orw}=0.10, S_w=0.90) respectively. Changes in PP amplitude are dominated by changes in saturation whereas changes in PS could either be due to changes in both pressure and saturation or changes in pressure only. Points mark variation at the gas cap (OG) and at the OWC (OW). For PP the changes in gas displacing oil and water displacing oil are in opposite directions whereas the changes are in the same direction for PS.*

could not be seen on the towed streamer legacy RMS amplitude could now be seen on the minimum amplitude map. Anomaly A is the main producing reservoir whereas anomalies B and C are the undrilled potential reservoirs. There is an increase in PP amplitude whereas the PS amplitude (Figure 1) decreases significantly in the main reservoir and slightly in the undrilled reservoir compartments. Attempts to interpret the production-induced changes of PP and PS are discussed in the following sections through petroelastic predictions, simulation and seismic modelling.

Petroelastic modelling predictions

Modelling is performed in order to understand how changes in pore pressure and saturation in the oil leg, impact on the PP and PS amplitudes. It is anticipated that V_P is to be affected by both pressure and saturation, whilst V_S is dominated by pressure to first order. Thus the PS data could have a stronger response to pressure than saturation. To confirm this intuition, the seismic velocities are calculated using a 28% porosity with densities and rock elastic moduli taken from the study of Pennington (2000) and the rock-frame pressure sensitivity relations of MacBeth (2003) with parameters suited to an unconsolidated Gulf of Mexico sandstone (Table 1). This rock-frame is then saturated by one of the following scenarios, namely: (a) oil saturated (S_o=0.85, S_{wc}=0.15); (b) oil displaced by gas and subsequent gas cap formation (S_g=0.75, S_{org}=0.10, S_{wc}=0.15); (c) water from aquifer replacing produced oil (S_{orw}=0.10, S_w=0.90) (at the reservoir pressure and temperature) using the requisite fluid properties and then Gassmann's equations, these defining the end-member regimes for cells in this particular reservoir model.

In Figure 2, the modelled PP and PS reflection amplitudes are plotted as a function of increasing effective pressures (and hence decreasing pore pressures) bracketing the Teal South reservoir conditions. The figure shows that for PP the effect of saturation is generally up to three times larger than the effect of pressure, with the largest changes being for gas. Points $\overrightarrow{OG}$ and $\overrightarrow{OW}$ are plotted on Figure 2 according to different locations in the reservoir. The first set $\overrightarrow{OG}$ corresponds to the exsolution of gas from oil and subsequent gas cap expansion. These indicate that whilst there is a production-related increase in PP amplitude, it is predicted that PS will show a slight decrease or no change in amplitude. In some cases, the effects of pore pressure drop may cancel out the saturation effects. The second set $\overrightarrow{OW}$ represent parts of the reservoir near to the oil-water contact, where oil is replaced by water (excepting the residual oil saturation). Here the amplitude decreases as the OWC rises upwards in both cases. These conclusions remain valid provided the rock-frame pressure-sensitivity parameters stay within the envelope of the database by MacBeth (2003) for reservoir and outcrop sands.

© 2003 EAGE

First Break September '03 06-08-2003 12:19 Pagina 13

Initial reservoir model and parameter assignment

The interpreted horizon picked from seismic was used as the structural model for building a reservoir model. There is one horizontal producer well (D10) completed in the 4500 ft sand and another well (D8) penetrating the sand but completed in the 6700 ft sand. With only one well going through the sand, there are more uncertainties in determining the fluid contacts and the NTG and porosity distribution across the reservoir. In order to get a more realistic model, we have to find a way of mapping the fluid contacts, porosity and NTG distribution using seismic which will act as input into our reservoir model. The technique for getting the fluid contact maps is discussed by Al-Naamani and MacBeth (2003).

The porosity distribution map is acquired by normalising the towed-streamer legacy RMS amplitude map (Figure 1) and rescaling it such that the maximum is 28%. The amplitude maps of OBC I and II at 100 Hz (Figure 3), after spectral decomposition, show that the turbidite sand unit is now seen to be made up of a series of smaller individual sands at this higher resolution. These could be high NTG channels. From these maps, the NTG values are calculated by rescaling the amplitudes such that the sub-channels have NTG equal to one, whereas the inter-channel facies are assigned NTG values lower than one but also proportional to the rescaled amplitudes. The GOC and OWC are clearly seen on the fluid contact maps from OBC I and II at Teal South (Figure 3). It is observed that the OWC is not regular and does not necessarily follow the horizon contours. This may be due to the heterogeneity of the reservoir. The movement of the OWC between OBC I and II surveys is approximately 3 m as derived from contact maps and thus the movement appears to be quite small. This can be explained as water drive being moderate during the solution gas drive phase of production. The OOWC has been fixed at the value for OBC I, this being consistent with the history match OOWC of Christie et al. (2002).

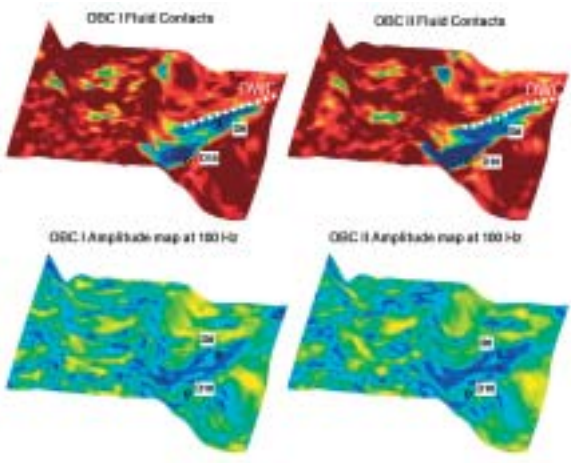

Figure 3 *Fluid contact and amplitude maps at 100 Hz, after spectral decomposition, for OBC I and OBC II. Between the two surveys, the expansion of gas cap and movement of OWC could be observed. The channels within the turbidite sand can be clearly seen on the amplitude map. These could be high NTG channels incised in the turbidite sheet.*

History matching

Figure 4 shows the flowchart that describes the steps of the history matching. Pennington et al. (2001) suggested that there was a pressure communication between blocks E and F which led to the 'little neighbour' reservoir (anomaly B)

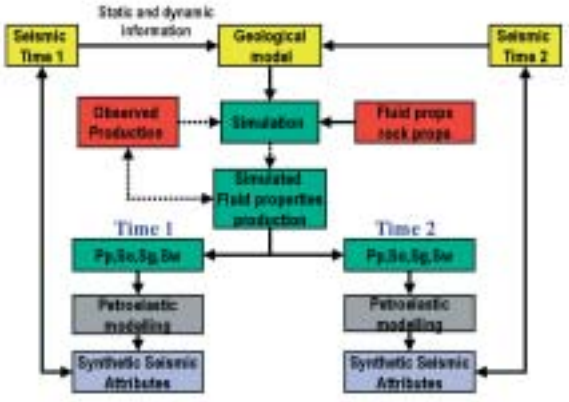

Figure 4 *Flowchart showing the procedure for 4D-4C seismic history match which includes production history match. The simulated saturation and pore pressure are used to generate time-lapse synthetics using 1D AVO seismic modeling for both PP and PS via petroelastic modelling.*

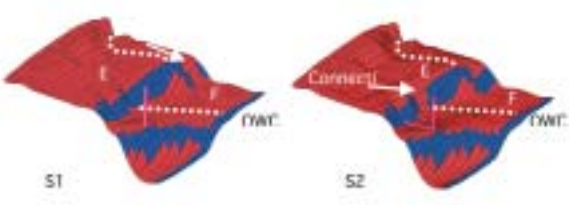

Figure 5 *Scenarios for the reservoir model showing different pressure connections between blocks E and F. S1 Connection between the water sands (bottom layer) and S2 Connection between the oil sands (top layer). The production takes place in block F but this induces a pressure decrease in block E through a pressure connection. The flow between blocks E and F is prevented by assigning zero transmissibility values along the fault plane except in the cells across the fault plane that links the two blocks.*

© 2003 EAGE

First Break September '03 06-08-2003 12:20 Pagina 14

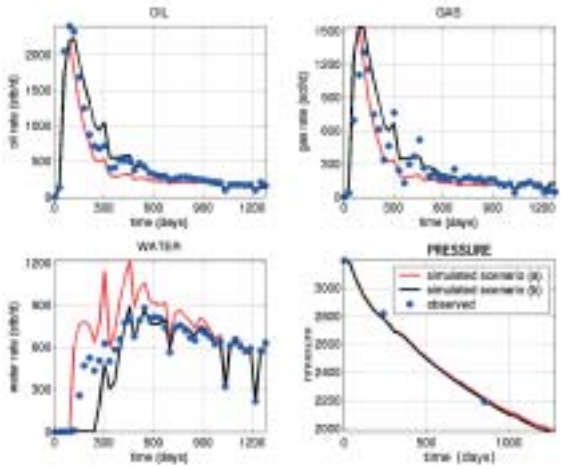

Figure 6 *Production history match for Teal South for both scenarios. The red line denotes the simulated production for scenario S1, black line denotes the simulated production for scenario S2 and the blue dots represent the actual production. For both scenarios, there is good match between the simulated and the actual production.*

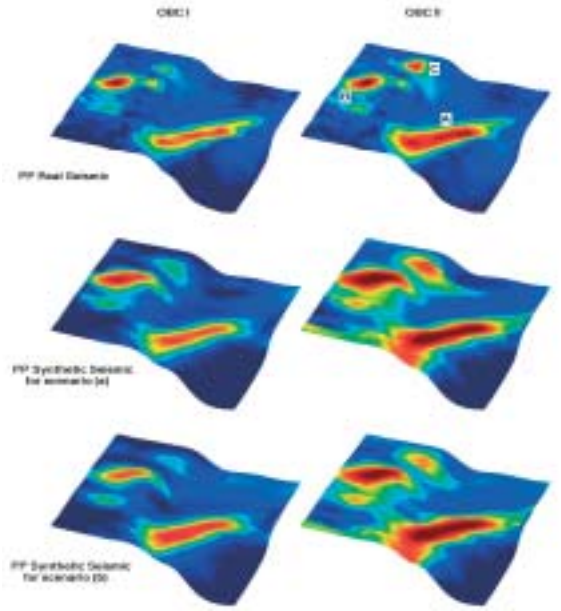

Figure 7 *Comparison between PP real and synthetic amplitude maps for OBC I and OBC II. The amplitudes are in agreement with what is observed in the real data. Anomalies B and C show time-lapse signature due to production from the main reservoir as pressure depletes through a pressure communication path. The anomalies B and C for scenario S1 are 20% brighter than those of scenario S2, which is what is observed in the real data.*

exhibiting a time-lapse signature. We examine two pressure connection scenarios between blocks E and F (Figure 5) in order to assess time-lapse signature in the sands B and C. The flow between blocks E and F is prevented by assigning zero transmissibility values along the fault plane except in the cells across the fault plane that links the two blocks. These cells act as a pressure connection between the water sands for scenario S1 and between the oil sands for scenario S2 at the bottom and top layers of the model respectively.

The simulator is constrained by the Teal South production history expressed in terms of daily production rate of oil, gas or water and averaged monthly. For both scenarios, Figure 6 shows how the simulator was able to reproduce the production history of the 4500 ft sand reservoir. The simulated fluid saturation and pore pressure, from the time of OBC I (July 1997) and OBC II (April 1999), are used to generate time-lapse synthetics for each location using 1D AVO seismic modelling for both PP and PS via petroelastic modelling. For both scenarios, there is brightening in PP amplitude (Figure 7) consistent with what is observed in the real seismic and as predicted by petroelastic modelling. Although the production histories for both scenarios were reproduced by the simulator, anomalies B and C for scenario S1 are 20% brighter than those of scenario S2 in the

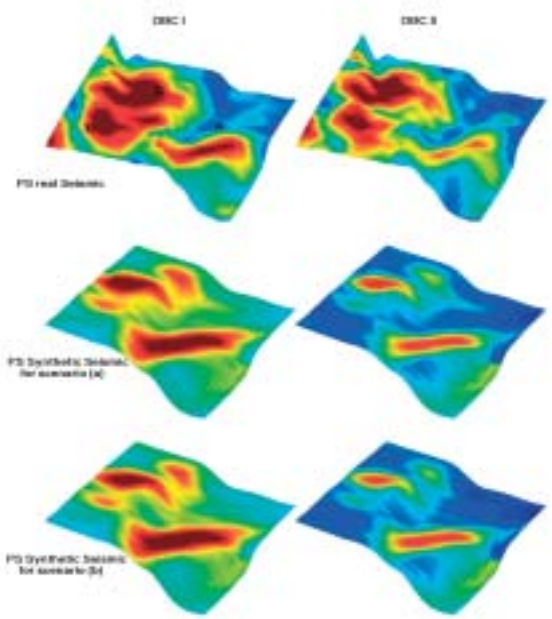

Figure 8 *Comparison between PS real and synthetic amplitude maps. There is a decrease in amplitude between the two surveys consistent with what is observed in the real data. The undrilled area (anomalies B and C) has a difference in character between real and synthetic seismic.*

© 2003 EAGE

First Break September '03 06-08-2003 12:20 Pagina 15

synthetic PP amplitude maps, which is what is observed in the real data. The PP results suggest that the pressure connection between blocks E and F is closer to the water sands connection.

There is virtually no difference between scenarios S1 and S2 for the PS synthetic amplitude maps, suggesting PS has no power to discriminate between these situations. However, relative amplitudes between anomalies do hold additional information. Both real and synthetic PS amplitude maps show dimming with the exception of anomaly C whose amplitude in real data virtually does not change, which could be due to the saturation cancelling the pressure effects (Figure 2). These observations suggest that there was a greater change in pore pressure in sands A and C than sand B, suggesting that there is a good pressure connection between sands A and C but not B. The PS data therefore adds value in assessing overall pressure communication between individual sand units in this particular reservoir.

Conclusions

The reservoir model has been history matched using production and 4D-4C seismic. The PP seismic attributes have been used as an input into the reservoir model. Two pressure connection scenarios have been examined in order to understand why the undrilled reservoir compartments show time-lapse signature. For both scenarios, the synthetic and real PP seismic amplitudes show overall good agreement. Pressure connection between the water sands of two fault blocks matches the observed time-lapse signature most closely. The synthetic and real PS seismic amplitudes show a good agreement as far as time-lapse signature is concerned although the undrilled reservoir reveals some differences. By jointly analysing the impact of pore pressure and saturation changes on PP and PS, the seismic can be used to infer reservoir connectivity.

Acknowledgements

The authors would like to acknowledge PDO for funding the studentship of Ali Al-Naamani. They would also like to thank Mike Christie and Karl Stephen for their help with the simulations.

References

Al-Naamani, A. and MacBeth, C. [2002] Joint interpretation of the time-lapse P-P and P-S response of a thin-bed reservoir. *72nd SEG Annual International Meeting*, Expanded Abstracts.

Al-Naamani, A. and MacBeth, C. [2003] Constraining the reservoir model of a turbidite reservoir using production and 4D seismic. *73rd SEG Annual International Meeting*, Expanded Abstracts.

Alexander, L.L., and Flemings, P. B.[1995] Geologic evolution of a Plio-Pleistocene salt withdrawal Mini-Basin: Eugene Island Block 330, Offshore Louisiana. *AAPG Bulletin.,* **79**, 1737-1756.

Christie, M., MacBeth, C., and Subbey, S. [2002] Multiple history-matched models for Teal South. *The Leading Edge* **21**, 286-289.

MacBeth, C. [2003] A classification for the pressure-sensitivity properties of a sandstone rockframe. *Geophysics,* In Press.

Pennington, W. [2000] 'Do no harm!' - Seismic petrophysical aspects of time-lapse monitoring. *70th SEG Annual International Meeting*, Expanded Abstracts..

Pennington, W.D., Acevedo, H., Haataja, J. I. and Minaeva, A. [2001] Seismic time-lapse surprise at Teal South: That little neighbor reservoir is leaking!. *The Leading Edge* **20**, 1172-1175.

© 2003 EAGE